

The Role of the $\Delta(1920)$ Resonance for Kaon Production in Heavy Ion Collisions

K. Tsushima*, S.W. Huang[†] and Amand Faessler

Institut für Theoretische Physik, Universität Tübingen
Auf der Morgenstelle 14, D-72076 Tübingen, F. R. Germany

Abstract

The long mean free path of K^+ mesons in nuclear matter makes this particle a suitable messenger for the dynamics of nucleus-nucleus reactions at intermediate energies (100 MeV to 3 GeV per nucleon). A prerequisite for this is the knowledge of the elementary production cross sections $\pi N \rightarrow \Sigma K$. Here these cross sections are studied for the first time with the explicit inclusion of the relevant baryon resonances up to 2 GeV as intermediate states. The baryon resonances – $N(1710) I(J^P) = \frac{1}{2}(\frac{1}{2}^+)$, $N(1720) \frac{1}{2}(\frac{3}{2}^+)$ and $\Delta(1920) \frac{3}{2}(\frac{3}{2}^+)$ – are taken into account coherently in the calculations of the $\pi N \rightarrow \Sigma K$ process. (We refer to this model as the ‘resonance model’.) Also $K^*(892) \frac{1}{2}(1^-)$ vector meson exchange is included. It is shown that the total cross sections for different channels of the $\pi N \rightarrow \Sigma K$ reactions, i.e. $\pi^+ p \rightarrow \Sigma^+ K^+$, $\pi^- p \rightarrow \Sigma^- K^+$, $\pi^+ n \rightarrow \Sigma^0 K^+$ ($\pi^- p \rightarrow \Sigma^- K^+$) and $\pi^0 p \rightarrow \Sigma^0 K^+$ differ not only by absolute values but also by their energy dependence. This shape differences are due to the mixture of the isospin $I = 3/2$ $\Delta(1920)$ with isospin $I = 1/2$ nucleon resonances. However, this $I = 3/2$ resonance does not give a contribution to the $\pi N \rightarrow \Lambda K$ reactions. So the shapes of the total cross sections $\pi N \rightarrow \Lambda K$ for different isospin projections are the same. In spite of this, such cross sections averaged over different isospin projections in the same multiplet are often used for studies of kaon production in heavy-ion collisions. Here we give an explicit separate parametrization of the cross sections for each channel $\pi N \rightarrow \Sigma K$, which are calculated in this work. The total cross section for $\pi^- p \rightarrow \Sigma^- K^+$ which runs through different $I = 3/2$ and $I = 1/2$ resonances can be well reproduced by the present model.

*Supported by DFG under contract No. Fa 67/14-1

[†]Supported by GSI under contract No. 06 Tü 736

Because kaons (K^+) have a long mean free path inside the nucleus, one believes that they are good messengers to provide information about the high density and temperature phase of the heavy ion collisions [1, 2]. Furthermore, they can be also sensitive probes for the nuclear equation of state (EOS) [3]. For these reasons, many studies of kaon production in heavy ion collisions have been performed both theoretically and experimentally [1]-[13].

In most theoretical studies of the kaon production in heavy ion collisions by either the Vlasov-Uehling-Uhlenbeck approach (VUU) [4], or by “quantum” molecular dynamics (QMD) [5, 6], however, the kaon elementary production cross sections in free space parametrized by J. Randrup and C. M. Ko [12] for $B_1 B_2 \rightarrow B_3 Y K$, and by J. Cugnon and R. M. Lombard [13] for $\pi N \rightarrow Y K$ are widely used. Here B stands for either the nucleon or the $\Delta(1232)$, Y stands for either the Σ or the Λ , respectively. Although there exists a relatively long history for kaon production studies, not many investigations have been performed for the elementary process [14].

On the other hand, due to recent high precision data, we have now rich and accurate informations on the baryon resonances, on quantum numbers, on decay modes, on decay rates and so on [15, 16]. Thus, it is now adequate and necessary to incorporate these resonances in calculations of the elementary cross section for kaon production. There are some works which include such baryon resonances in kaon production studies [10, 11]. In these, simple parametrizations by Breit-Wigner forms are given. Since the $\pi N \rightarrow \Lambda K$ amplitudes arising from the relevant resonances are not calculated, the interferences among these resonances is not included. Furthermore, the $\pi N \rightarrow \Sigma K$ reactions are not investigated in these publications.

The first purpose of the present article is to present model calculations of $\pi N \rightarrow \Sigma K$ at intermediate energies, which take into account the nucleon- ($I = 1/2$) and the delta ($I = 3/2$) resonances up to 2 GeV in the intermediate states. By intermediate energies we mean that the center-of-mass energy \sqrt{s} of the πN ranges from the threshold of kaon production to about 3 GeV. Kaon production by pions on nucleons are so-called secondary processes in heavy ion collisions, which are known to give about a 30 % contribution to kaon production in the intermediate or low energy region [9].

The energy dependence of the total cross sections and the peak positions (e.g. $\pi^- p \rightarrow \Lambda K^0$ reaction [17]) show that the s-channel resonance processes given in fig. 1 are dominant for the $\pi N \rightarrow Y K$ reactions. (See also the experimental data given in fig. 3 (a).)

According to the compilation of the “Review of Particle Properties” [15, 16], the resonances $N(1710) I(J^P) = \frac{1}{2}(\frac{1}{2}^+)$, $N(1720) \frac{1}{2}(\frac{3}{2}^+)$ and $\Delta(1920) \frac{3}{2}(\frac{3}{2}^+)$ give the main s-channel contributions to the reactions $\pi N \rightarrow \Sigma K$. Although it is expected to be small (and it will be shown so) we consider the lightest $K^*(892) \frac{1}{2}(1^-)$ vector meson for t-channel K^* exchange contributions.

The second purpose of this article is to focus on the role of the $\Delta(1920)$ resonance for the $\pi N \rightarrow \Sigma K$ reaction, since this resonance has isospin $I = 3/2$ and contributes differently from those of the isospin $I = 1/2$ nucleon resonances. Because the experimental data [15, 16] show that this resonance does not decay to ΛK , we will not discuss the $\pi N \rightarrow \Lambda K$ reactions in the present article. A detailed study including the ΛK channel will be reported elsewhere [18].

In order to see the different isospin structure of the processes represented by (a), (b), (c) and (d) in fig. 1, we consider the following schematic structures in isospin space,

$$(a) : \quad (\bar{K} \vec{\Sigma} \cdot \vec{\tau} N(1710)) (\bar{N}(1710) \vec{\tau} \cdot \vec{\phi} N), \quad (1)$$

$$(b) : \quad (\bar{K} \vec{\Sigma} \cdot \vec{\tau} N(1720)) (\bar{N}(1720) \vec{\tau} \cdot \vec{\phi} N), \quad (2)$$

$$(c) : \quad (\bar{K} \vec{\Sigma} \cdot \vec{\mathcal{I}}^\dagger \Delta(1920)) (\bar{\Delta}(1920) \vec{\mathcal{I}} \cdot \vec{\phi} N), \quad (3)$$

$$(d) : \quad (\bar{K} \vec{\tau} K^*(892) \cdot \vec{\phi}) (\bar{K}^*(892) \vec{\Sigma} \cdot \vec{\tau} N), \quad (4)$$

where $\vec{\mathcal{I}}$ is the transition operator defined by

$$\vec{\mathcal{I}}_{Mm} = \sum_{\ell=\pm 1,0} (1\ell \frac{1}{2} m | \frac{3}{2} M) \hat{e}_\ell^*,$$

and $\vec{\tau}$ are the Pauli matrices. $N, N(1710), N(1720)$ and $\Delta(1920)$ stand for the fields of $N(938), N(1710), N(1720)$ and $\Delta(1920)$ resonances. They are expressed by $\bar{N} = (\bar{p}, \bar{n})$, similarly to the nucleon resonances, and $\bar{\Delta}(1920) = (\bar{\Delta}(1920)^{++}, \bar{\Delta}(1920)^+, \bar{\Delta}(1920)^0, \bar{\Delta}(1920)^-)$. The fields appearing in eqs. (1) - (3) are related to the physical representations as follows: $K^T = (K^+, K^0)$, $\bar{K} = (K^-, \bar{K}^0)$, $K^*(892)^T = (K^*(892)^+, K^*(892)^0)$, $\bar{K}^*(892) = (K^*(892)^-, \bar{K}^*(892)^0)$, $\pi^\pm = \frac{1}{\sqrt{2}}(\phi_1 \mp i\phi_2)$, $\pi^0 = \phi_3$, $\Sigma^\pm = \frac{1}{\sqrt{2}}(\Sigma_1 \mp i\Sigma_2)$, $\Sigma^0 = \Sigma_3$, where the superscript T means transposition operation. The pseudoscalar meson fields are defined as annihilating (creating) the physical particle (anti-particle) states. $SU(2)$ isospin symmetry is assumed for each doublet or multiplet.

Without factors arising from isospin structure, we define the amplitudes $\mathcal{M}_a, \mathcal{M}_b, \mathcal{M}_c$ and \mathcal{M}_d corresponding to each diagram (a), (b), (c) and (d) given in fig. 1. Then each amplitude contributing to the $\pi N \rightarrow \Sigma K$ reactions (which will be referred as ‘different channels’) is given by,

$$\begin{aligned} \mathcal{M}_c + 2\mathcal{M}_d \text{ for} & \quad \pi^+ p \rightarrow \Delta(1920)^{++}, K^*(892)^0 \rightarrow \Sigma^+ K^+ \\ \text{and} & \quad \pi^- n \rightarrow \Delta(1920)^-, K^*(892)^+ \rightarrow \Sigma^- K^0, \end{aligned} \quad (5)$$

$$\begin{aligned} 2(\mathcal{M}_a + \mathcal{M}_b + \frac{1}{6}\mathcal{M}_c) \text{ for} & \quad \pi^- p \rightarrow n(1710), n(1720), \Delta^0(1920) \rightarrow \Sigma^- K^+ \\ \text{and} & \quad \pi^+ n \rightarrow p(1710), p(1720), \Delta^+(1920) \rightarrow \Sigma^+ K^0, \end{aligned} \quad (6)$$

$$\begin{aligned} \sqrt{2}(\mathcal{M}_a + \mathcal{M}_b - \frac{1}{3}\mathcal{M}_c - \mathcal{M}_d) & \quad \text{for } \pi^+ n \rightarrow p(1710), p(1720), \Delta(1920)^+, K^*(892)^0 \rightarrow \Sigma^0 K^+ \\ \text{and } \pi^0 p \rightarrow p(1710), p(1720), \Delta(1920)^+, K^*(892)^0 & \rightarrow \Sigma^+ K^0, \end{aligned} \quad (7)$$

$$\begin{aligned} -\sqrt{2}(\mathcal{M}_a + \mathcal{M}_b - \frac{1}{3}\mathcal{M}_c - \mathcal{M}_d) & \quad \text{for } \pi^0 n \rightarrow n(1710), n(1720), \Delta(1920)^0, K^*(892)^+ \rightarrow \Sigma^- K^+ \\ \text{and } \pi^- p \rightarrow n(1710), n(1720), \Delta(1920)^0, K^*(892)^+ & \rightarrow \Sigma^0 K^0, \end{aligned} \quad (8)$$

$$\begin{aligned}
& \mathcal{M}_a + \mathcal{M}_b + \frac{2}{3}\mathcal{M}_c + \mathcal{M}_d \\
& \text{for } \pi^0 p \rightarrow p(1710), p(1720), \Delta(1920)^+, K^*(892)^+ \rightarrow \Sigma^0 K^+ \\
& \text{and } \pi^0 n \rightarrow n(1710), n(1720), \Delta(1920)^+, K^*(892)^0 \rightarrow \Sigma^0 K^0. \quad (9)
\end{aligned}$$

Here the intermediate resonance states are explicitly written between the two arrows pointing to the right. Note that $I = 1/2$ t-channel K^* meson exchanges do not contribute to the channel given by eq. (6) due to the isospin structure. From eqs. (5) - (9) one can see that the $\Delta(1920)$ (represented by the amplitude \mathcal{M}_c) contributes to different channels in different ways than the other $N(1710)$ and $N(1720)$ resonances (represented by the amplitudes \mathcal{M}_a and \mathcal{M}_b) and $K^*(892)$ exchange (represented by \mathcal{M}_d).

This means that the $\Delta(1920)$ resonance modifies the energy dependence of the cross section for the different channels of $\pi N \rightarrow \Sigma K$ reactions. (Except for the reactions given in eq. (7) and eq. (8).) This is completely different from the $\pi N \rightarrow \Lambda K$ reactions, where only the isospin $I = 1/2$ nucleon resonances can contribute in s-channel and there is no t-channel K^* exchange contributions.

Before proceeding to the specific model calculations, we can roughly estimate the $\Delta(1920)$ resonance contributions to the total cross sections of each different channel defined by eqs.(6) - (9) neglecting $K^*(892)$ exchange contribution. The experimental total cross section $\sigma(\pi^+ p) (\propto |\mathcal{M}_c^2|)$ for the $\pi^+ p \rightarrow \Sigma^+ K^+$ channel has a peak with a value of about 0.7 mb located around $\sqrt{s} = 1.92$ GeV as seen from fig. 3 (a). We assume the $\Delta(1920)$ contribution is dominant, due to the experimental branching ratios [15, 16], and the fact that only charge $2e$ intermediate states are allowed. Then the incoherent contributions of this $\Delta(1920)$ resonance to each total cross section at this peak position may be estimated as follows: $\frac{1}{9}|\mathcal{M}_c|^2 \propto \frac{1}{9}\sigma(\pi^+ p) \simeq 0.08$ mb for the channels defined by eq. (6), $\frac{2}{9}|\mathcal{M}_c|^2 \propto \frac{2}{9}\sigma(\pi^+ p) \simeq 0.16$ mb for the channels defined by eqs. (7) and (8), and $\frac{4}{9}|\mathcal{M}_c|^2 \propto \frac{4}{9}\sigma(\pi^+ p) \simeq 0.32$ mb for the channels defined by eq. (9), respectively. Thus, this $\Delta(1920)$ resonance can give sizable contributions to each channel. From this estimate we expect that the cross sections for the different channels in the $\pi N \rightarrow \Sigma K$ reactions will be different from each other not only in absolute values but also in its energy dependence.

In order to illustrate this argument more clearly, we perform here model calculations for these cross sections. Effective interaction Lagrangians for the processes represented by fig. 1 are used:

$$\mathcal{L}_{\pi NN(1710)} = -ig_{\pi NN(1710)} \left(\bar{N}(1710)\gamma_5\vec{\tau}N \cdot \vec{\phi} + \bar{N}\vec{\tau}\gamma_5N(1710) \cdot \vec{\phi} \right), \quad (10)$$

$$\mathcal{L}_{\pi NN(1720)} = \frac{g_{\pi NN(1720)}}{m_\pi} \left(\bar{N}^\mu(1720)\vec{\tau}N \cdot \partial_\mu\vec{\phi} + \bar{N}\vec{\tau}N^\mu(1720) \cdot \partial_\mu\vec{\phi} \right), \quad (11)$$

$$\mathcal{L}_{\pi N\Delta(1920)} = \frac{g_{\pi N\Delta(1920)}}{m_\pi} \left(\bar{\Delta}^\mu(1920)\vec{\mathcal{I}}N \cdot \partial_\mu\vec{\phi} + \bar{N}\vec{\mathcal{I}}^\dagger\Delta^\mu(1920) \cdot \partial_\mu\vec{\phi} \right), \quad (12)$$

$$\mathcal{L}_{K\Sigma N(1710)} = -ig_{K\Sigma N(1710)} \left(\bar{N}(1710)\gamma_5\vec{\tau} \cdot \vec{\Sigma}K + \bar{K}\vec{\Sigma} \cdot \vec{\tau}\gamma_5N(1710) \right), \quad (13)$$

$$\mathcal{L}_{K\Sigma N(1720)} = \frac{g_{K\Sigma N(1720)}}{m_K} \left(\bar{N}^\mu(1720)\vec{\tau} \cdot \vec{\Sigma}\partial_\mu K + (\partial_\mu\bar{K})\vec{\Sigma} \cdot \vec{\tau}N^\mu(1720) \right), \quad (14)$$

$$\mathcal{L}_{K\Sigma\Delta(1920)} = \frac{g_{K\Sigma\Delta(1920)}}{m_K} \left(\bar{\Delta}^\mu(1920)\vec{\mathcal{I}} \cdot \vec{\Sigma}\partial_\mu K + (\partial_\mu\bar{K})\vec{\mathcal{I}}^\dagger \cdot \vec{\mathcal{I}}\Delta^\mu(1920) \right), \quad (15)$$

$$\mathcal{L}_{K^*(892)\Sigma N} = -g_{K^*(892)\Sigma N} \left(\bar{N} \gamma^\mu \vec{\tau} \cdot \vec{\Sigma} K_\mu^*(892) + \frac{\xi}{m_N + m_\Sigma} \bar{N} \sigma^{\mu\nu} \vec{\tau} \cdot \vec{\Sigma} \partial_\mu K_\nu^*(892) + \text{h.c.} \right), \quad (16)$$

$$\mathcal{L}_{K^*(892)K\pi} = if_{K^*(892)K\pi} \left(\bar{K} \vec{\tau} K_\mu^*(892) \cdot \partial^\mu \vec{\phi} - (\partial^\mu \bar{K}) \vec{\tau} K_\mu^*(892) \cdot \vec{\phi} \right) + \text{h.c.}, \quad (17)$$

where ξ is the ratio of the tensor coupling constant to the vector coupling constant. The spin 3/2 Rarita-Schwinger fields $\psi^\mu = N^\mu(1720)$, $\Delta^\mu(1920)$ with mass m satisfy the set of equations [19],

$$(i\gamma \cdot \partial - m)\psi^\mu = 0, \quad (18)$$

$$\gamma_\mu \psi^\mu = 0, \quad (19)$$

$$\partial_\mu \psi^\mu = 0. \quad (20)$$

There are several problems in order to treat spin 3/2 massive particles and spin 1/2 and 3/2 resonances consistently. They are discussed in great detail in refs. [20], and [21, 22, 23]. The problems discussed in these references are, for example, connected with the uniqueness of the free Lagrangian for the massive spin 3/2 particles, with the propagator having a definite spin 3/2 projection, with the unitarity due to the widths inserted into the propagators of the resonances, and so on. There seems to be according to Benmerrouche et al. [20] also a problem with the constraint to the off shell propagator of spin 3/2 particles suggested by Peccei [22]. Although keeping these discussions in mind we must use a phenomenological specific form for the propagators of the resonances. We use for the propagators $S_F(p)$ of the spin 1/2 and $G^{\mu\nu}(p)$ of the spin 3/2 resonances,

$$S_F(p) = \frac{\gamma \cdot p + m}{p^2 - m^2 + im\Gamma^{full}}, \quad (21)$$

$$G^{\mu\nu}(p) = \frac{P^{\mu\nu}(p)}{p^2 - m^2 + im\Gamma^{full}}, \quad (22)$$

with

$$P^{\mu\nu}(p) = -(\gamma \cdot p + m) \left[g^{\mu\nu} - \frac{1}{3} \gamma^\mu \gamma^\nu - \frac{1}{3m} (\gamma^\mu p^\nu - \gamma^\nu p^\mu) - \frac{2}{3m^2} p^\mu p^\nu \right], \quad (23)$$

where m and Γ^{full} stand for the mass and the full decay width of the corresponding resonance.

Without factors arising from isospin space, the explicit amplitudes \mathcal{M}_a , \mathcal{M}_b , \mathcal{M}_c and \mathcal{M}_d corresponding diagrams (a), (b), (c) and (d) depicted in fig. 1 are given as follows:

$$\mathcal{M}_a = \frac{-g_{\pi NN(1710)} g_{K\Sigma N(1710)}}{p^2 - m_{N(1710)}^2 + im_{N(1710)} \Gamma_{N(1710)}^{full}} \bar{u}_\Sigma(p_\Sigma) \gamma_5 (\gamma \cdot p + m_{N(1710)}) \gamma_5 u_N(p_N), \quad (24)$$

$$\mathcal{M}_b = \frac{g_{\pi NN(1720)} g_{K\Sigma N(1720)}}{m_\pi m_K} \frac{p_{K\mu} p_{\pi\nu}}{p^2 - m_{N(1720)}^2 + im_{N(1720)} \Gamma_{N(1710)}^{full}} \bar{u}_\Sigma(p_\Sigma) P_{N(1720)}^{\mu\nu}(p) u_N(p_N), \quad (25)$$

$$\mathcal{M}_c = \frac{g_{\pi N \Delta(1920)} g_{K \Sigma \Delta(1920)}}{m_\pi m_K} \frac{p_{K\mu} p_{\pi\nu}}{p^2 - m_{\Delta(1920)}^2 + im_{\Delta(1920)} \Gamma_{\Delta(1920)}^{full}} \bar{u}_\Sigma(p_\Sigma) P_{\Delta(1920)}^{\mu\nu}(p) u_N(p_N), \quad (26)$$

$$\mathcal{M}_d = \frac{f_{K^*(892)K\pi} g_{K^*(892)\Sigma N}}{(p_\Sigma - p_N)^2 - m_{K^*(892)}^2} \bar{u}_\Sigma(p_\Sigma) \left[\gamma_\mu - i \frac{\xi}{m_N + m_\Sigma} \sigma_{\alpha\mu} (p_\Sigma - p_N)^\alpha \right] \cdot (p_\pi + p_K)_\nu \left(g^{\mu\nu} - \frac{(p_\Sigma - p_N)^\mu (p_\Sigma - p_N)^\nu}{m_{K^*(892)}^2} \right) u_N(p_N), \quad (27)$$

where $u_N(p_N)$ and $u_\Sigma(p_\Sigma)$ are the spinors of the nucleon and the Σ , with the four momenta p_N and p_Σ , respectively. (See fig. 1.)

We also need to determine the coupling constants appearing in the Lagrangians given by eqs. (10) - (17). In order to include the finite size effects of hadrons, form factors (denoted by $F(q)$ and $F_{K^*(892)K\pi}(q)$ below) will be introduced. These form factors must be multiplied to each vertex of the interaction. Thus, the absolute values of the coupling constants except for $g_{K^*(892)\Sigma N}$ are determined from the branching ratios in the rest frame of the resonances:

$$\Gamma(N(1710) \rightarrow BP) = 3 \frac{g_{PBN(1710)}^2 F^2(q(m_{N(1710)}, m_B, m_P))}{4\pi} \cdot \frac{(E_B - m_B)}{m_{N(1710)}} q(m_{N(1710)}, m_B, m_P), \quad (28)$$

$$\Gamma(B^* \rightarrow BP) = D \frac{g_{PBB^*}^2 F^2(q(m_{B^*}, m_B, m_P))}{12\pi} \frac{(E_B + m_B)}{m_{B^*} m_P^2} q^3(m_{B^*}, m_B, m_P), \quad (29)$$

$$\Gamma(K^*(892) \rightarrow K\pi) = 3 \frac{f_{K^*(892)K\pi}^2 F_{K^*(892)K\pi}^2(q(m_{K^*(892)}, m_K, m_\pi))}{4\pi} \cdot \frac{2}{3m_{K^*(892)}^2} q^3(m_{K^*(892)}, m_K, m_\pi), \quad (30)$$

with

$$F(q) = \frac{\Lambda_C^2}{\Lambda_C^2 + q^2}, \quad F_{K^*(892)K\pi}(q) = Cq \exp(-\beta q^2), \quad (31)$$

$$q(x, m_B, m_P) = \frac{1}{2x} \left[(x^2 - (m_B + m_P)^2) (x^2 - (m_B - m_P)^2) \right]^{1/2}, \quad (32)$$

where $E_B = \sqrt{m_B^2 + \vec{p}_B^2}$ ($q = |\vec{p}_B|$), B^* stands for either the $N(1720)$ or the $\Delta(1920)$ resonance, B stands for either the $N(938)$ or the Σ , and P stands for either the π or the K , respectively. Also the corresponding masses are represented by m_{B^*} , m_B and m_P . In the above, $F(q)$ is the form factor with a cut off parameter Λ_C , and $D = 3$ and $D = 1$ should be assigned to the $N(1720)$ and the $\Delta(1920)$, respectively. The $K^*(892)K\pi$ vertex form factor is taken from ref. [24]. In evaluating the cross sections in the center-of-mass frame of the πN system, each coupling constant g_{PBB^*} , $g_{K^*(892)\Sigma N}$ and $f_{K^*(892)K\pi}$ appearing in the eqs. (24) - (27) must be replaced by $g_{PBB^*} \rightarrow g_{PBB^*} F(q(\sqrt{s}, m_B, m_P))$, $g_{K^*(892)\Sigma N} \rightarrow g_{K^*(892)\Sigma N} F((\vec{q}_f - \vec{q}_i))$ and $f_{K^*(892)K\pi} \rightarrow f_{K^*(892)K\pi} F_{K^*(892)K\pi}(\frac{1}{2}(\vec{q}_f - \vec{q}_i))$,

with $\vec{p}_B = -\vec{p}_P$, $q = |\vec{p}_B|$, $|\vec{q}_f| = q(\sqrt{s}, m_\Sigma, m_K)$, $|\vec{q}_i| = q(\sqrt{s}, m_N, m_\pi)$ and s being the Mandelstam variable. (See also the caption of fig. 2.)

The cut off parameters used for the numerical calculations are: $\Lambda_C = 0.8$ GeV for the $N(1710)$ and the $N(1720)$ resonances, $\Lambda_C = 0.5$ GeV for the $\Delta(1920)$ resonance and $\Lambda_C = 1.2$ GeV for the $K^*(892)\Sigma N$ vertex, respectively. The parameters C and β in $F_{K^*(892)K\pi}$ are $C = 2.72$ fm and $\beta = 8.88 \times 10^{-3}$ fm² used in ref. [24].

We first discuss the $\pi^+p \rightarrow \Sigma^+K^+$ channel displayed in fig 3 (a). The experimental data are given with error bars [17]. Note that only the $\Delta(1920)$ contributes to this reaction in the s-channel. (See eq. (5).) The dashed line stands for the result using the coupling constants determined from the branching ratios and eqs. (29) - (32), and the fitted value for $g_{K^*(892)\Sigma N}$ which will be explained later. This shows a large underestimation – of about a factor 12 – if branching ratio data are used to determine the coupling constants for the baryon resonances. The $K^*(892)$ exchange contribution to this total cross section gives an almost constant background as a function of energy, and thus must be small so that it is consistent with the experimental data. The total cross section is mainly due to the $\Delta(1920)$ resonance in the present model, thus the two coupling constants relevant for this resonance (see eq. (29) and Table 1) are rescaled in order to fit the data in fig. 3 (a). The coupling constant $g_{K^*(892)\Sigma N}$ is chosen to fit the tail of this cross section with zero tensor coupling for $K^*(892)\Sigma N$ interaction, i.e. $\xi = 0$ in eq. (16), and the rescaled coupling constants for $\Delta(1920)$ are used. This value for $g_{K^*(892)\Sigma N}$ is used for the results represented by the dashed line in fig. 3 (a). The result using the rescaled coupling constants and the value $g_{K^*(892)\Sigma N}$ fitted as described above is represented by the solid line in fig. 3 (a). This set of coupling constants will be also used later.

In the following calculations, two different sets of the coupling constants will be used. For set 1 we use the rescaled coupling constants for the $\Delta(1920)$ resonance and the fitted coupling constant $g_{K^*(892)\Sigma N}$. All the other coupling constants are determined from the branching ratios. The results obtained using the coupling constants determined fully by the experimental branching ratios and the same value of $g_{K^*(892)\Sigma N}$ as case 1 will be referred as set 2. Explicit values of the coupling constants obtained and the experimental branching ratios are listed in table 1.

Hereafter, we will discuss the K^+ production channels only. Corresponding arguments for the K^0 production channels are valid as seen from eqs. (5) - (9).

The calculated total cross sections for the other channels are displayed in figs. 3(b) - 3(d). The contributions of the interference terms appearing in these channels are included as follows: Since the branching ratios determine only the square of the coupling constants, all eight possible relative signs among the interference terms are evaluated. Then that sign combination which reproduces the experimental data best for $\pi^-p \rightarrow \Sigma^-K^+$ is selected. (See fig. 3 (b).) After fixing the relative signs among the interference terms for this reaction, all other channels are evaluated with this fixed relative signs.

First we discuss the global features of figs. 3(b) - 3(d). It is clear that the total cross sections of different channels show a different energy dependence, for both set 1 and set 2. This different energy dependence is due to the $\Delta(1920)$ resonance contributions as already mentioned in the text. Without the $\Delta(1920)$ resonance contributions, they all have the same energy dependence but different absolute values. Thus, this isospin $I = 3/2$ $\Delta(1920)$ resonance differentiates the energy dependences of the total cross sections for the

different channels in the $\pi N \rightarrow \Sigma K$ reactions.

Next, it is interesting to look at the $\pi^- p \rightarrow \Sigma^- K^+$ channel in fig. 3 (b). The experimental data are also given with error bars [17]. The parameters of set 1 can reproduce the second peak of the experimental data around the total center-of-mass energy $\sqrt{s} = 1.95$ GeV. But the parameters of set 2 fail to reproduce this second peak. This second peak described correctly by the parameters of set 1 is again the consequence of the isospin $I = 3/2$ $\Delta(1920)$ resonance contribution. Thus, this fact shows the superiority of the parameters of the set 1 for the present study. The success of set 1 and the failure of set 2 to explain the $\pi^+ p \rightarrow \Sigma^+ K^+$ and $\pi^- p \rightarrow \Sigma^- K^+$ data simultaneously might indicate that there exist other resonances with masses around 1.9 GeV and isospin $I = 3/2$ which can give large enough contributions to reproduce the $\pi^+ p \rightarrow \Sigma^+ K^+$ total cross section, and also give the second peak of the reaction $\pi^- p \rightarrow \Sigma^- K^+$.

In figs. 3(c) and 3(d), the calculated total cross sections for the $\pi^+ n \rightarrow \Sigma^0 K^+$ and $\pi^0 n \rightarrow \Sigma^- K^+$, and $\pi^0 p \rightarrow \Sigma^0 K^+$ are shown. Set 1 results for $\pi^0 p \rightarrow \Sigma^0 K^+$ should be reliable prediction.

Since the energy-dependent form of the decay widths is not unique, energy independent decay widths are used in the propagators for the present study. To see the effects of energy-dependent decay widths in the propagators for the resonances, some calculations have also been done using an energy dependent decay width $\Gamma(s) = \Gamma^{full} \left(\frac{q(\sqrt{s}, m_B, m_P)}{q(m, m_B, m_P)} \right)^{2L+1}$, where L is the orbital angular momentum quantum number of the corresponding resonance. (See also eq. (32) and fig. 2.) It turned out that this energy dependence of the decay width does not give significant effects on the energy dependence of the cross sections.

For kaon production in heavy ion collisions, we give parametrizations of the total cross sections $\sigma(\pi N \rightarrow \Sigma K)$ for each separate channel based on set 1. They are:

$$\sigma(\pi^+ p \rightarrow \Sigma^+ K^+) = \frac{0.03591(\sqrt{s} - 1.688)^{0.9541}}{(\sqrt{s} - 1.890)^2 + 0.01548} + \frac{0.1594(\sqrt{s} - 1.688)^{0.01056}}{(\sqrt{s} - 3.000)^2 + 0.9412} \quad \text{mb}, \quad (33)$$

$$\sigma(\pi^- p \rightarrow \Sigma^- K^+) = \frac{0.009803(\sqrt{s} - 1.688)^{0.6021}}{(\sqrt{s} - 1.742)^2 + 0.006583} + \frac{0.006521(\sqrt{s} - 1.688)^{1.4728}}{(\sqrt{s} - 1.940)^2 + 0.006248} \quad \text{mb}, \quad (34)$$

$$\sigma(\pi^+ n \rightarrow \Sigma^0 K^+) \quad \text{and}$$

$$\sigma(\pi^0 n \rightarrow \Sigma^- K^+) = \frac{0.05014(\sqrt{s} - 1.688)^{1.2878}}{(\sqrt{s} - 1.730)^2 + 0.006455} \quad \text{mb}, \quad (35)$$

$$\sigma(\pi^0 p \rightarrow \Sigma^0 K^+) = \frac{0.003978(\sqrt{s} - 1.688)^{0.5848}}{(\sqrt{s} - 1.740)^2 + 0.006670} + \frac{0.04709(\sqrt{s} - 1.688)^{2.1650}}{(\sqrt{s} - 1.905)^2 + 0.006358} \quad \text{mb}, \quad (36)$$

where, all parametrizations given above should be understood to be zero below threshold for $\sqrt{s} \leq 1.688$ GeV. These parametrizations are especially useful for kaon production simulation codes for those channels where no experimental data are available.

To summarize, we studied the $\pi N \rightarrow \Sigma K$ reactions focusing on the role of the $\Delta(1920)$ resonance, and presented for the first time theoretical calculations. The results obtained show that the isospin $I = 3/2$ $\Delta(1920)$ resonance has a significant role to distinguish the energy dependence of the total cross sections for different channels

of the reactions $\pi N \rightarrow \Sigma K$. We gave parametrizations of the total cross sections for each separate channel obtained for set 1 parameters, where the coupling constants for the $\Delta(1920)$ resonance and $g_{K^*(892)K\pi}$ are fitted to reproduce $\pi^+p \rightarrow \Sigma^+K^+$ and other coupling constants are determined from decay ratios. The good agreement obtained with set 1 parameters and the failure of the set 2 parameters might indicate that there exist other resonances with masses around 1.9 GeV and isospin $I = 3/2$, which contribute to the $\pi^+p \rightarrow \Sigma^+K^+$ channel to explain the total cross section, and reproduce simultaneously also the second peak of $\pi^-p \rightarrow \Sigma^-K^+$.

Acknowledgement: The authors express their thanks to Prof. R. Vinh Mau and Prof. H. Mütter for useful discussions. We thank also Prof. K. W. Schmid who provided us the code used to adjust the parameters in the present study.

References

- [1] S. Schnetzer et al., Phys. Rev. Lett. 49 (1982) 989; S. Nagamiya, Phys. Rev. Lett. 49 (1982) 1383.
- [2] T. Abbott et al., Phys. Rev. Lett. 64 (1990) 847; A. Berglund et al., Nucl. Phys. B 166 (1980) 25; M. Aguilar-Benitez et al., Z. Phys. C 6 (1980) 109; P. A. Baker et al., Phys. Rev. Lett. 40 (1979) 678; T. M. Knasel et al., Phys. Rev. D 11 (1975) 1; S. R. Deans et al., Nucl. Phys. B 96 (1975) 90; D. J. Candlin et al., Nucl Phys. B 238 (1984) 477; K. W. Bell et al., Nucl. Phys. B 222 (1983) 389.
- [3] J. Aichelin and C. M. Ko, Phys. Rev. Lett. 55 (1985) 2661.
- [4] W. Cassing, V. Metag, U. Mosel and K. Niita, Phys. Rep. 188 (1990) 363.
- [5] J. Aichelin, Phys. Rep. 202 (1991) 235.
- [6] G. Q. Li, A. Faessler and S. W. Huang, Progresses in particles and nuclear physics 31 (1993) 159.
- [7] C. M. Ko, Z. G. Wu, L. H. Xia and G. E. Brown, Phys. Rev. Lett. 66 (1991) 2577.
- [8] A. Lang, W. Cassing, U. Mosel and K. Weber, Nucl. Phys. A 541 (1992) 507; S. W. Huang et al., Phys. Lett. B 298 (1993) 41; G. Hartnack, J. Jänicke and J. Aichelin, preprint, Universite de Nantes, Rapport Interne LPN-93-11 (1993).
- [9] T. R. Halemane and A. Z. Mekjian, Phys. Rev. C 25 (1982) 2398; H. W. Barz and H. Iwe, Phys. Lett. B 143 (1984) 55; W. Cassing et al., Phys. Lett. B 238 (1990) 25; A. A. Sibirstev and M. Buescher, Z. Phys. A 347 (1994) 191.

- [10] G. E. Brown, C. M. Ko, Z. G. Wu and L. H. Xia, Phys. Rev. C 43 (1991) 1881; H. W. Barz and H. Iwe, Nucl Phys. A 453 (1986) 728; V. Pantuev, Phys. Lett. B 281 (1992) 20.
- [11] C. M. Ko, X. S. Fang and Y. Z. Zhang, International workshop XXI on Gross properties of nuclei and nuclear excitations, ed. by Ferdmeier, (1993) 29.
- [12] J. Randrup and C. M. Ko, Nucl. Phys. A 343 (1980) 519; Nucl. Phys. A 411 (1983) 537.
- [13] J. Cugnon and R. M. Lombard, Nucl. Phys. A 422 (1984) 635.
- [14] E. Ferrari, Phys. Rev. 120 (1960) 988; T. Yao, Phys. Rev. 125 (1962) 1048.
- [15] Particle Data Group, Phys. Rev. D 45 (1992).
- [16] Particle Data Group, Phys. Lett. B 239 (1990) 1.
- [17] A. Baldini, V. Flamino, W. G. Moorhead and D. R. O. Morrison, *Landolt-Börnstein, Numerical Data and Functional Relationships in Science and Technology*, Vol. 12, ed. by H. Schopper, (Springer-Verlag, 1988).
- [18] S. W. Huang, K. Tsushima, Amand Faessler, E. Lehmann and Rajeev K. Puri, in preparation; K. Tsushima, S. W. Huang and Amand Faessler, in preparation.
- [19] See, for example, Y. Takahashi, *An Introduction to Field Quantization*, (Pergamon Press, 1969); D. Lurié, *Particles and Fields*, (John Wiley & Sons, 1968).
- [20] M. Benmerrouche, R. M. Davidson and Nimai C. Mukhopadhyay, Phys. Rev. C 39 (1989) 2339.
- [21] H. T. Williams, Phys. Rev. C 31 (1985) 2297.
- [22] R. D. Peccei, Phys. Rev. 176 (1968) 1812.
- [23] A. Aurila and H. Umezawa, Phys. Rev. 182 (1969) 1682; K. Johnson and E. C. G. Sudarshan, Ann. Phys. 13 (1961) 126; H. Watanabe, H. Shimodaira and S. Kamefuchi, Nucl. Phys. B 2 (1967) 360.
- [24] C. Gobbi, F. Iachello and D. Kusnezov, Yale University preprint (1994) PACS numbers: 13.25.+m, 11.30.Na, 12.40.Aa.

Table 1: Calculated and fitted coupling constants

$B^*(\text{resonance})$	$\Gamma(\text{MeV})$	$\Gamma_{N\pi}(\%)$	$g_{B^*N\pi}^2$	$\Gamma_{\Sigma K}(\%)$	$g_{B^*\Sigma K}^2$
$N(1710)$	100	15.0	2.57	6.0	$4.50 \times 10^{+1}$
$N(1720)$	150	15.0	5.27×10^{-2}	3.5	3.15
$\Delta(1920)$ (set 1)	–	–	(1.44)	–	(3.83)
$\Delta(1920)$ (set 2)	200	12.5	4.17×10^{-1}	2.0	1.11
$f_{K^*(892)K\pi}^2$			$g_{K^*(892)\Sigma N}^2$		
6.89×10^{-1} ($\Gamma=50$ MeV, $\Gamma_{K\pi} = 100\%$)			2.03×10^{-1}		

Table 1

The calculated or fitted coupling constants and the data used for the calculations. The values in brackets stand for the coupling constants obtained by fitting to the total cross section for the $\pi^+p \rightarrow \Sigma^+K^+$ reaction (set 1). The value of $g_{K^*(892)\Sigma N}^2$ is the fitted value to the $\pi^+p \rightarrow \Sigma^+K^+$ channel when zero tensor coupling for $K^*(892)\Sigma N$ interaction ($\xi = 0$) is applied and the rescaled coupling constants for $\Delta(1920)$ are used.

Figure captions

Fig. 1

The processes contributing to the $\pi N \rightarrow \Sigma K$ reactions. The diagrams are corresponding to the different intermediate resonance states: (a) : $N(1710) I(J^P) = \frac{1}{2}(\frac{1}{2}^+)$, (b) : $N(1720) \frac{1}{2}(\frac{3}{2}^+)$, (c) : $\Delta(1920) \frac{3}{2}(\frac{3}{2}^+)$ and (d) : t-channel $K^*(892)$ exchange, respectively.

Fig. 2

The formation or decay vertex of the resonance B^* appearing in the amplitudes eqs. (24) - (26). Here B^* stands for the resonances $N(1710)$, $N(1720)$ and $\Delta(1920)$. B stands for the baryons N and Σ . P stands for the pseudoscalar mesons π and K . The variable given in each bracket stands for the four momentum of each particle. In the center-of-mass frame of the baryon B and the pseudoscalar meson P , they are $p_{B^*}^\mu = (\sqrt{s}, \vec{0})$, $p_B^\mu = (E_B, \vec{p}_B)$ and $p_P^\mu = (E_P, -\vec{p}_B)$ with $|\vec{p}_B| = q(\sqrt{s}, m_B, m_P)$ defined by eq. (32).

Fig. 3 (a)

The calculated total cross sections for the $\pi^+ p \rightarrow \Sigma^+ K^+$ ($\pi^- n \rightarrow \Sigma^- K^0$) reaction. The solid line and the dashed line stand for the set 1 and set 2 parameters, respectively. Set 1 are the relevant coupling constants for $\Delta(1920)$ and $g_{K^*(892)K\pi}$ adjusted to the cross section $\pi^+ N \rightarrow \Sigma^+ K^+$ with the $\Delta(1920)$ as an s-channel intermediate state resonance and other coupling constants are determined from the branching ratios. Set 2 uses the same value of $g_{K^*(892)K\pi}$ as that of set 1 and other coupling constants determined only from the branching ratios.

Fig. 3 (b)

The calculated total cross sections for the $\pi^- p \rightarrow \Sigma^- K^+$ ($\pi^+ n \rightarrow \Sigma^+ K^0$) reaction. See the caption of fig. 3 (a) for further explanations.

Figs. 3 (c)

The calculated total cross sections for the $\pi^+ n \rightarrow \Sigma^0 K^+$ and $\pi^0 n \rightarrow \Sigma^- K^+$ ($\pi^0 p \rightarrow \Sigma^+ K^0$ and $\pi^- p \rightarrow \Sigma^0 K^0$) reactions. See the caption of fig. 3 (a) for further explanations.

Figs. 3 (d)

The calculated total cross sections for the $\pi^0 p \rightarrow \Sigma^0 K^+$ ($\pi^0 n \rightarrow \Sigma^0 K^0$) reaction. See the caption of fig. 3 (a) for further explanations. No experimental data are known.

Fig. 1

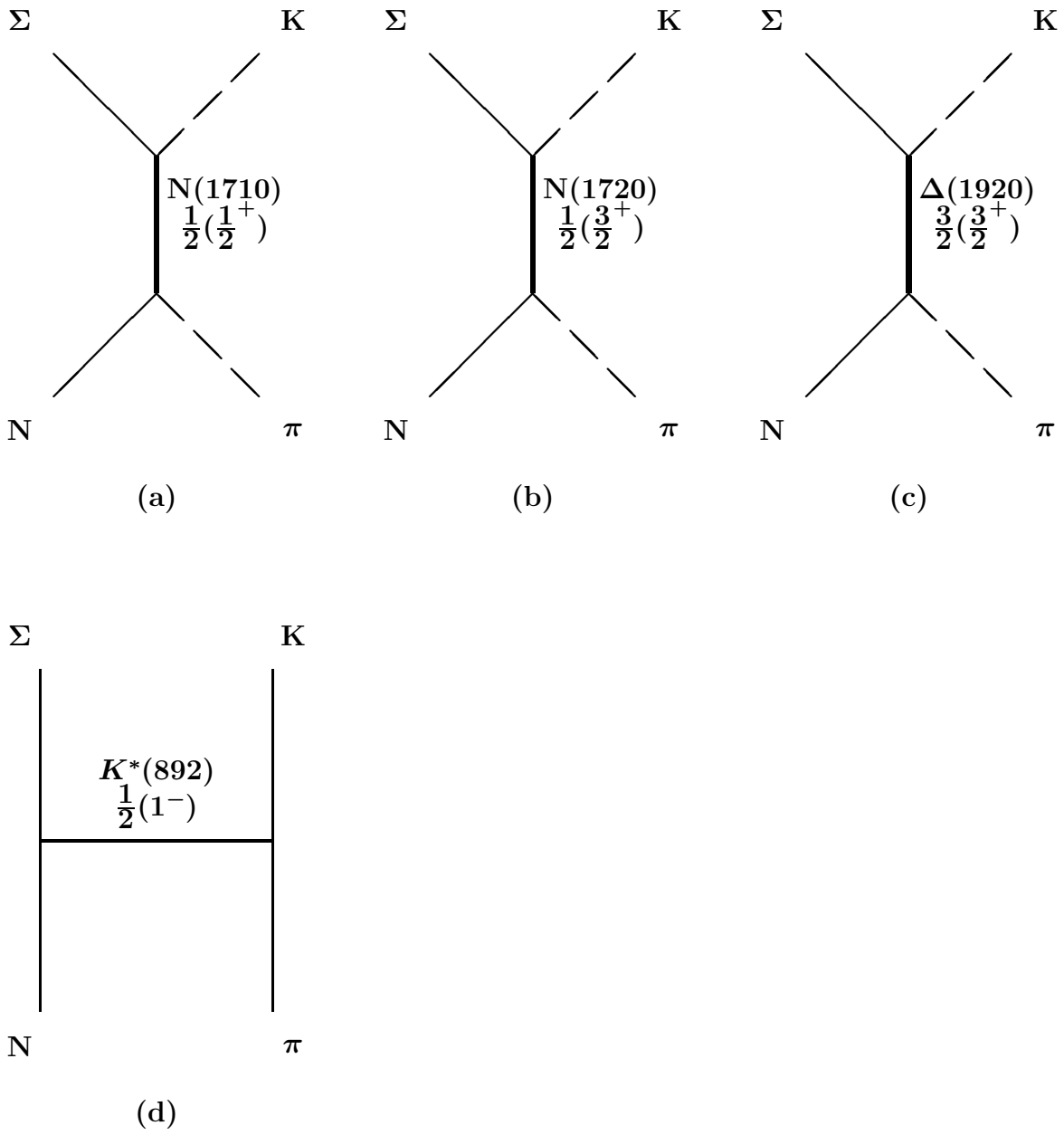
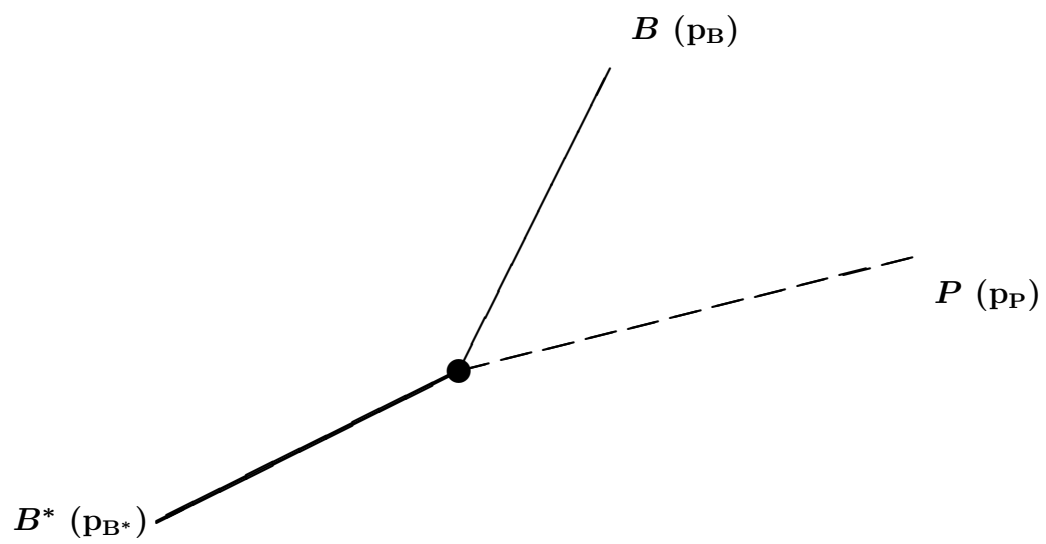


Fig. 2



This figure "fig1-1.png" is available in "png" format from:

<http://arxiv.org/ps/nucl-th/9407021v3>

This figure "fig2-1.png" is available in "png" format from:

<http://arxiv.org/ps/nucl-th/9407021v3>

This figure "fig3-1.png" is available in "png" format from:

<http://arxiv.org/ps/nucl-th/9407021v3>

This figure "fig4-1.png" is available in "png" format from:

<http://arxiv.org/ps/nucl-th/9407021v3>